Available online: journal.ipb.ac.id/index.php/jphpi

EFFECT OF SULFURIC ACID TREATMENT IN CELLULOSE NANOCRYSTALS EXTRACTION FROM Sargassum sp. SEAWEED

Dina Fransiska[1,2*], Sabina Hastiana[3], B. Boy Rahardjo Sidartha[3], Azizah Intan Pangesty[1], Mochamad Chalid[1], Dedi Priadi[1], Gilles Ausias[4], Hari Eko Irianto[2*]

[1]Department of Metallurgical and Materials Engineering, Faculty of Engineering, University of Indonesia, UI Campus, Depok Indonesia 16424

[2]Marine and Terrestrial Bioindustry Research Center, Earth and Maritime Research Organization, National Research and Innovation Agency,
720 Building, KST BJ Habibie, Serpong, Tangerang Selatan Indonesia 15314

[3]Faculty of Biotechnology, Atma Jaya University
Babarsari st. No.44, Janti, Caturtunggal, Yogyakarta Indonesia 55281

[4]IRDL-UMR CNRS 6027, Univ. Bretagne Sud,
Ctre de Recherche Christian Huygens, Rue de Saint-Maudé, Lorient France 56100

Submitted: 8 May 2025/Accepted: 9 September 2025
*Correspondence: kustiaz@apps.ipb.ac.id

How to cite (APA Style 7th): Fransiska, D., Hastiana, S., Sidartha, B. B. R., Pangesty, A. I., Chalid, M., Priadi, D., Ausias, G., & Irianto, H. E. (2025). Effect of sulfuric acid treatment in cellulose nanocrystals extraction from *Sargassum* sp. seaweed. *Jurnal Pengolahan Hasil Perikanan Indonesia,* 28(9), 772-788. http://dx.doi.org/10.17844/y5x3as39

Abstract

Sargassum sp. is a type of brown seaweed often found in tropical waters, but it has not been optimally used. The high cellulose content of *Sargassum* sp. can be used to produce cellulose nanocrystals (CNC). CNC can act as a bionanocomposite-reinforced nanomaterial. This study aimed to determine the most effective sulfuric acid concentration for extracting cellulose nanocrystals from *Sargassum* sp. CNC was extracted from *Sargassum* sp. using acid hydrolysis and sonication. The sulfuric acid concentration was varied to 30, 40, 50, and 60%. CNC was characterized using Fourier-transform infrared spectroscopy (FTIR), X-ray diffraction (XRD), and thermogravimetric analysis (TGA). FTIR analysis confirmed the presence of characteristic CNC functional group peaks, including C–O–C (~1160 cm^{-1}), C–O (~1050–1030 cm^{-1}), and β-(1→4)-glycosidic C–H (~897 cm^{-1}) as the CNC fingerprint. The FTIR findings indicated that the CNC extracted by sulfuric acid hydrolysis differed significantly from the raw *Sargassum* sp. material. Additionally, the XRD results showed that acid hydrolysis substantially affected the amorphous regions of cellulose. With 40% acid hydrolysis, the XRD analysis showed the highest CNC degree of 77.6%. Thermal analysis using TGA and DTG revealed that cellulose nanocrystals treated with 40% acid hydrolysis yielded CNC with enhanced thermal stability, exhibiting a maximum thermal decomposition temperature of 369.60°C. CNC isolated from *Sargassum* sp. cellulose has the potential to serve as a suitable source for manufacturing nanocomposites in various applications, such as pharmaceuticals, food packaging, and biomedical fields.

Keywords: brown algae, crystallinity, FTIR, hydrolysis, sonication

Efek Perlakuan Asam Sulfat pada Ekstraksi Selulosa Nanokristal dari Rumput Laut *Sargassu*m sp.

Abstrak

Sargassum sp. adalah jenis rumput laut cokelat yang banyak ditemukan di perairan tropis, namun belum dimanfaatkan secara optimal. Kandungan selulosa yang tinggi dalam *Sargassum* sp. dapat digunakan untuk menghasilkan selulosa nanokristal (CNC). CNC dapat digunakan sebagai bahan nano penguat bionanokomposit. Penelitian ini bertujuan untuk menentukan konsentrasi asam sulfat yang optimum untuk mengekstraksi nanokristal selulosa dari *Sargassum* sp. CNC dari *Sargassum* sp. diekstraksi menggunakan

http://dx.doi.org/10.17844/y5x3as39

metode hidrolisis asam dan sonikasi. Variasi konsentrasi asam sulfat pada proses ekstraksi CNC, yaitu 30, 40, 50, dan 60%. Karakterisasi CNC dilakukan menggunakan spektroskopi inframerah (FTIR), difraksi sinar-X (XRD), dan analisis termogravimetri (TGA). Analisis FTIR mengonfirmasi keberadaan puncak gugus fungsi khas CNC, termasuk C–O–C (\~1160 cm^{-1}), C–O (\~1050–1030 cm^{-1}), dan C–H β-(1→4)-glikosidik (\~897 cm^{-1}) sebagai sidik jari CNC. Hal ini menunjukkan bahwa CNC yang diekstraksi melalui hidrolisis asam sulfat memiliki perbedaan yang signifikan dibandingkan dengan bahan baku *Sargassum* sp. Selain itu, hasil XRD menunjukkan bahwa hidrolisis asam berpengaruh pada berkurangnya daerah amorf pada CNC. Analisis XRD menunjukkan tingkat CNC tertinggi sebesar 77,6% pada hidrolisis asam sulfat 40%. Analisis termal menggunakan TGA dan DTG menunjukkan bahwa CNC yang diproses dengan hidrolisis asam sulfat 40% menghasilkan CNC dengan stabilitas termal yang meningkat, menunjukkan suhu dekomposisi termal sebesar 369,60 °C. CNC yang diisolasi dari *Sargassum* sp. berpotensi sebagai bahan pembuatan nanokomposit dalam berbagai aplikasi, misalnya bidang farmasi, pengemasan makanan, dan biomedis.

Kata kunci: alga cokelat, FTIR, hidrolisis, kristalinitas, sonikasi

INTRODUCTION

Indonesia, as an archipelagic country, has a large maritime area with a coastline of 81,290 km (Hikmawati et al.,2023). This extensive coastline provides abundant marine resources, including seaweed. Among the diverse seaweed species, *Sargassum* sp., a type of brown macroalgae (*Phaeophyceae*), is commonly found along the coastal waters of Indonesia. However, its potential remains largely underutilized, and it is often regarded as waste that disrupts fishing activities and maritime navigation (Khansa *et al.,* 2024). *Sargassum* sp. has a rich chemical composition, containing valuable compounds such as alginic acid, fucoidan, fucoxanthin, phenolics (Erniati *et al*., 2024; Ramlan *et al*., 2024), and cellulose (Safitri *et al.,* 2021). The cellulose content of *Sargassum* sp. ranges from 23.97% to 35.22%(Taslim *et al.,* 2017), indicating significant potential for value-added applications.

Marine biomass, such as *Sargassum* sp., is a promising raw material for producing cellulose nanocrystals (CNC), which are renewable and biodegradable nanomaterials. CNC exhibit exceptional properties, including high mechanical strength, biocompatibility, high crystallinity, and large surface area, making them highly suitable for a wide array of applications, ranging from reinforcement in polymer composites and biodegradable packaging to drug delivery systems (Doh & Whiteside, 2020; George & Sabapathi, 2015). Although several studies have explored CNCs derived from marine algae biomass, such as *Dictyota bartayreisana* (Murugesan et al.,2024), *Gelidiella acerosa* (Singh *et al.,* 2017), and *Cladophora glomerata* (Plianwong & Sirirak, 2024), relatively few studies have investigated CNCs from marine sources such as *Sargassum*. Initial studies have indicated that CNC derived from *Sargassum* and other marine algae can enhance the mechanical and thermal properties of biopolymer films (Doh, 2020; El Achaby *et al.,* 2018). However, the extraction processes, particularly the optimization of acid hydrolysis parameters, remain inadequately explored.

CNC extraction typically involves acid hydrolysis to selectively remove the amorphous regions of cellulose, thereby isolating the crystalline domains of the cellulose (Muljani *et al.,* 2023). Mechanical treatment, such as ultrasonication, is often used afterward to reduce the particle size to the nanoscale (Saputri & Sukmawan, 2020). One critical factor affecting CNC yield and quality is the concentration of sulfuric acid used for hydrolysis. Several studies have reported the potential of brown seaweed (Doh *et al.,* 2020; Murugesan *et al.,* 2024) as a source of CNC for hydrolysis using sulfuric acid. However, the chemical composition and characteristics of *Sargassum* are highly dependent on its growing location, making it important to evaluate the potential of this species in Indonesian waters, particularly those around Yogyakarta.

Therefore, this study aimed to determine the most effective sulfuric acid concentration for the hydrolysis of cellulose nanocrystals from *Sargassum* sp. to optimize the yield and enhance the quality of the resulting nanomaterials for potential

applications. The findings are expected to support the sustainable utilization of marine biomass and contribute to the development of high-performance and environmentally friendly nanomaterials.

MATERIALS AND METHODS

Preparation of Raw Materials

Sargassum sp. *was* supplied by Gunung Kidul Regency, Yogyakarta, Indonesia. *Sargassum* sp. *was* washed and dried in the sun for two days. *Dry Sargassum sp.* (moisture content: 10.50%) was ground using a grinder. and stored at room temperature before use in the extraction process (Doh et al.,2020). Commercial CNC was used as a positive control and obtained from CelluForce, Canada.

Pretreatment

The chemical solutions used were hydrochloric acid (HCl), sodium hydroxide (NaOH), potassium hydroxide (KOH), sodium hypochlorite (NaOCl), glacial acetic acid, hydrogen peroxide (H_2O_2), and sulfuric acid (H_2SO_4). All chemical solutions used were of technical grade. *Sargassum* sp. (20 g) was dissolved in 200 mL 0.2 M HCl and heated in a *water bath* at 30°C for 2 h. The sample was centrifuged at 15,000 ×g for 10 min. The residue was separated from the supernatant and re-suspended in 300 mL distilled water. The suspension was adjusted to pH 10 using 4% NaOH and heated in a water bath at 75°C for 3 h.

The heated sample was rinsed with water until a pH of 7 was reached, and then centrifuged at 15,000 ×g for 10 min. The residue was separated from the supernatant, dried in an oven at 65°C for 20 h, and then added to 350 mL of 10% KOH. The mixture was heated in a water bath at 80°C for 3 h. The heated sample was rinsed with tap water until a pH of 7 was reached, and 50 mL of 6.5% NaOCl solution was added. The suspension was stirred and left to stand for 30 min until the color of the sample brightened.

The sample was rinsed with tap water 3-4 times, and 300 mL of distilled water was added. Glacial acetic acid was added to adjust the pH to 5, and the sample was heated in a water bath at 75°C for 2 h. The heated sample was rinsed with distilled water until a pH of 7 was reached, and 20 mL of 10% H_2O_2 solution was added. The suspension was heated in a water bath at 80°C for 70 minutes, followed by 3-4 flushes with distilled water (Doh *et al.,* 2020).

Acid Hydrolysis

The wet pre-treated sample was added with 100 mL of H_2SO_4 (30, 40, 50, and 60%), and then heated in a water bath at 45°C for 30 min. The heated sample was added to 200 mL of cold water and centrifuged at 15,000 ×g for 10 min. The pellets were rinsed with tap water until pH 7 was reached, and then centrifuged at 15,000 ×g for 10 min (centrifugation was carried out twice).

The acid-hydrolyzed samples were added to distilled water and then toned using an ultrasonic device (UCD 250, Biomaisen, China) at a frequency of 20 KHz and an amplitude of 30% of the total power of 500 W for 15 min. CNC was freeze dried using a freeze dryer, the liquid sample was frozen at -80°C for 24 h and then subjected to high vacuum (0.05 mbar) for another 24 h.

Characterization

Yields

Yield is the ratio of the final weight of a product to the initial weight of a dry sample (Septiani *et al.,* 2017). The final weight of the sample was obtained by weighing the freeze-dried CNC, and the initial weight of the sample was obtained by weighing the *Sargassum* sp. powder.

Fourier transform infrared spectroscopy (FTIR)

The FTIR spectrum was obtained using ATR-FTIR (Nicolet iS 5 ATR iD5, Thermo Scientific, USA) in the range of 500–4000 cm^{-1}. Measurements were made at a scan resolution of 4 cm^{-1} (Nurhayati *et al.,* 2025).

X-ray diffraction (XRD)

The CNC crystallinity index was determined using XRD with Cu Kα radiation (λ = 1.54060 Å) in the range of 2θ 4° to 60°. The operating conditions were set at 40

http://dx.doi.org/10.17844/y5x3as39

kV and 25 mA. The crystallinity index was calculated using the Segal method, following the defined equation. The CNC crystallinity index was determined using XRD, using Cu Kα radiation (λ = 0.15406 nm) in the range of 2θ 4° to 60° with operating conditions set at 40 kV and 25 mA. The crystallinity index is calculated using the Segal method, following the specified equation (Doh *et al.,* 2020).

$$\text{Crystallinity index (\%)} = \frac{I_{200} - I_{am}}{I_{200}} \times 100$$

Note:

I_{200} = maximum intensity on the field (200) (2θ = 22,4°)

I_{am} = minimum intensity in the valley between the fields (200) dan (110) (2θ = 18,1°)

Thermogravimetric analysis (TGA)

The analysis was carried out under a nitrogen atmosphere (20 mL/min) with a heating rate of 10°C/min, covering a temperature range from 25°C to 500°C (Costa *et al.,* 2015).

Crystallite size

The crystallite size of the cellulose nanocrystals (CNCs) was determined using X-ray diffraction (XRD) analysis. The average crystallite size (D) was calculated using the Scherrer equation (Alam et al.,2024), based on the Full Width at Half Maximum (FWHM) of the most intense diffraction peak. The FWHM values were obtained by fitting the XRD peaks using Gaussian peak fitting in the Origin Learning for Student software.

$$D = \frac{K\lambda}{\beta \cos \theta}$$

Note:

D = average crystallite size (nm),

K = the shape factor (commonly taken as 0.9),

λ = the wavelength of the X-ray (0.15406 nm),

β = FWHM of the diffraction peak in radians,

θ = the Bragg angle corresponding to the peak.

Data Analysis

The FTIR, XRD, and TGA analyses were processed and analyzed using Excel and Origin software. Yield data were collected in triplicate and analyzed using one-way ANOVA at a significance level of $p<0.05$.

RESULT AND DISCUSSION

CNC Yield

Yield is defined as the ratio of the final weight of a product to the initial weight of the sample (Septiani *et al.,* 2017). The CNC of freeze-dried *Sargassum* sp. is shown in Figure 1. Based on Figure 1, it can be observed that the CNC extracted from *Sargassum* sp. is solid, white, odorless, and tasteless. These findings are in line with the statement that high-quality cellulose is usually powdered, white, and odorless (Pine *et al.,* 2021). While the CNC from *Sargassum* sp. does not show a powder shape but rather a dry solid form, which can be attributed to the freeze-drying process, causing the water to evaporate and the sample to become solid (Agustin & Wibowo, 2021). The white color of the CNC derived from *Sargassum* sp. is associated with the whitening process (Harpendi *et al.,* 2014).

The CNC yield for each treatment was calculated to determine the optimal H_2SO_4 concentration for producing the highest amount of CNC from *Sargassum* sp. Yield is an important indicator of extraction efficiency (Fransiska *et al.,* 2020). A graph depicting the CNC results for *Sargassum* sp. is presented in Figure 2.

Based on Figure 2, the CNC yield of *Sargassum* sp. ranged from 3.79±2.20% to 7.15±1.42%. The highest yield was achieved using 40% H_2SO_4, whereas the lowest yield was observed using 60% H_2SO_4. This yield is relatively low compared to that of CNCs derived from other brown, red, and green seaweeds. Doh *et al.* (2020) reported CNC yields of 25.8 ± 0.9% and 26.1±1.2% from *Sargassum fluitans* and *Laminaria japonica* (kombu), respectively. Similarly, Murugesan *et al.* (2024) found that *Dictyota bartayresiana*, a tropical brown seaweed species, yielded approximately 10% CNC under optimized acid hydrolysis conditions.

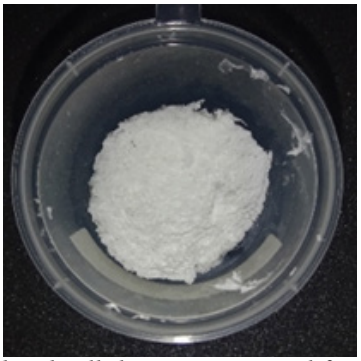

Figure 1 Freeze dried cellulose nano crystal from *Sargassum* sp.

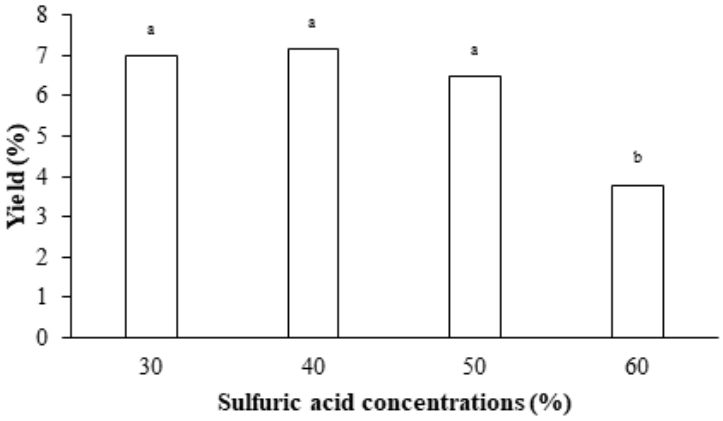

Figure 2 CNC yield from *Sargassum* sp. seaweed with varying H_2SO_4 concentrations

Previous research by Harahap *et al.* (2019) found a similar trend, with CNC corn cobs extracted using 45% H_2SO_4 yielding 16.98%, lower than the 36.48% yield obtained with 55% H_2SO_4. This can occur because low-concentration H_2SO_4 is less effective in breaking down all the amorphous parts of cellulose, causing many cellulose crystals to remain attached to the cellulose chain, resulting in a lower number of cellulose crystals.

Sulfuric acid (H_2SO_4) at a concentration of 30-50% is effective in removing amorphous cellulose, thus enabling the isolation of high amounts of crystalline cellulose. Higher yield values correlate with greater efficacy in producing large quantities of the desired product (Moranda *et al.,* 2018).

The extraction of Sargassum sp. using less than 60% H_2SO_4 can be attributed to an increase in the hydrogen bonds between the hydroxyl cellulose (OH) groups and water molecules. Hydrolysis using H_2SO_4 can split the hydrogen bonds in cellulose, resulting in a free OH group formation. The OH group in cellulose can bind to water molecules (Gian *et al.,* 2017). The binding of water molecules by OH groups increases the weight of the CNC, thereby increasing the percentage of results (Simarmata *et al.,* 2024).

The CNC yields extracted using 60% H_2SO_4 decreased because of the removal of the amorphous regions in the cellulose chain by H_2SO_4, leaving only crystalline regions (Effendi *et al.,* 2015). Sunardi *et al.* (2019) also reported a decrease in microcrystalline cellulose (MCC) yield with an increase in hydrochloric acid (HCl) concentration.

Fourier Transform Infrared Spectroscopy (FTIR) of CNC

FTIR spectroscopy was used to identify the functional groups present in the compounds. Each functional cluster has a unique infrared absorption frequency. Figure 3 presents the FTIR spectra of CNCs obtained at different hydrolysis concentrations are presented in Figure 3.

http://dx.doi.org/10.17844/y5x3as39

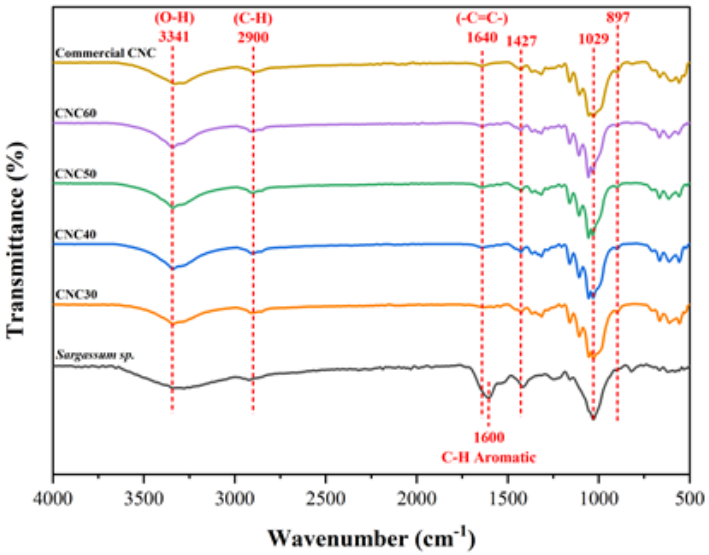

Figure 3 FTIR spectra of CNC commercial and CNC extracted from *Sargassum* sp. under different sulfuric acid hydrolysis concentration

The peak observed at 3341 cm^{-1} may be attributed to the O-H stretching of the hydroxyl group in cellulose. This aligns with the findings that OH stretching vibrations typically appear within the 3500–3200 cm^{-1} range (Theivandran *et al.,* 2015). Additionally, the peaks around 2900 cm^{-1} are attributed to the stretching vibrations of the CH groups (alkanes). This observation aligns with the fact that peaks in the 2900–2800 cm^{-1} range are characteristic of CH stretching, particularly from CH_3 and CH_2 groups (Topală *et al.,* 2017).

The peak at 1640 cm^{-1} shows a cluster vibration of -C=C-, which is in accordance with the statement by Theivandran *et al.* (2015) that peaks in the range of 1680-1640 cm^{-1} are associated with the stretching vibration of the -C=C- group in alkenes. The C=C group is a structural component of the aromatic ring in lignin (Pambudi *et al.,* 2017). The peak at 1600 cm^{-1} in the *Sargassum* sp. spectrum indicates the absorption of infrared radiation by the lignin aromatic CH group. This is in accordance with the statement of Natsir *et al.* (2022) that the vibration of the stretching of the CH group aromatic lignin occurs at approximately 1600 cm^{-1}.

The peaks at 1427 cm^{-1} and 1415 cm^{-1} correspond to the aromatic CC group vibrations. This is in accordance with the statement by Theivandran *et al.* (2015), who reported that the vibration of the CC group stretch in the aromatic ring structure occurs at 1500-1400 cm^{-1}. The peaks at 1366 cm^{-1} and 1314 cm^{-1} indicate CH cluster vibrations. Pangau *et al.* (2017) stated that peaks at 1369 cm^{-1} and 1327 cm^{-1} indicate CH group vibration of cellulose.

Peaks at 1159, 1108, 1059, and 1029 cm^{-1} show the stretching vibrations of the cellulose C-O-C group. This is in accordance with the statement of Bashar *et al.* (2019), who indicated that the peaks at 1160, 1110, 1060, and 1028 cm^{-1} indicate the vibration of the pyranos ring skeleton and glucose. Peaks at 897 cm^{-1} indicate CH group vibrations associated with β-glycosidic bonds, which is consistent with the statement by Abu-Thabit *et al.* (2020) that absorption at a peak of 895 cm^{-1} is associated with CH vibrations (specific anomeric vibrations of β-glycosidic bonds).

Lower transmission values correspond to higher absorption of infrared radiation by the functional groups in the compounds (Raturandang *et al.,* 2022). The transmission values of the functional groups are presented in Table 1.

The transmission values of CNC30, CNC40, CNC50, and CNC60 were lower than those of *Sargassum* sp. at 3341, 2900, 1366, 1314, 1159, 1108, 1056, 1029, and 897 cm^{-1}.

Table 1 Transmittance of CNC commercial and CNC extracted from *Sargassum* sp. under different sulfuric acid hydrolysis conditions

Wavenumber (cm^{-1})	Transmittance (T)						Functional group	Ref.
	CNC30	CNC40	CNC50	CNC60	Commercial CNC	*Sargassum* sp.		
3341	0.90	0.79	0.81	0.80	0.92	0.96	O-H stretch	(Theivandran *et al.*, 2015)
2900	0.96	0.92	0.93	0.93	0.96	0.98	C-H stretch	(Topală *et al.*, 2017)
1640	0.99	0.97	0.96	0.97	0.99	0.95	-C=C- stretch	(Theivandran *et al.*, 2015)
1600	0.98	0.98	0.98	0.98	0.99	0.94	C-H (Aromatic)	(Natsir *et al.*, 2022)
1427	0.96	0.93	0.94	0.94	0.97	0.96	C-C stretch (Aromatic)	(Theivandran *et al.*, 2015)
1415	0.97	0.95	0.96	0.96	0.98	0.96		
1366	0.95	0.92	0.93	0.93	0.96	0.98	C-H	(Umpuch, 2015)
1314	0.94	0.89	0.91	0.92	0.95	0.98		(Pangau *et al.*, 2017)
1203	0.99	0.97	0.97	0.96	0.98	0.98	C-O stretch	(Kusumaningsih *et al.*, 2022) (finger print)
1159	0.91	0.83	0.84	0.84	0.92	0.98	C-O-C	(Bashar *et al.*, 2019) (finger print)
1108	0.84	0.71	0.74	0.74	0.87	0.96		
1056	0.74	0.54	0.56	0.57	0.79	0.92		
1029	0.73	0.53	0.59	0.61	0.79	0.90		
897	0.96	0.96	0.97	0.98	0.96	0.99	C-H (β-glycosidic bond)	(Abu-Thabit *et al.*, 2020) (finger print)

http://dx.doi.org/10.17844/y5x3as39

This indicates a higher cellulose content in the 30%, 40%, 50%, and 60% samples. The high cellulose content indicates that the non-cellulose components (lignin, hemicellulose, alginate, etc.) were successfully reduced during the pretreatment stage, and cellulose was successfully extracted from *Sargassum* sp. using the acid hydrolysis method.

The O–H stretching band at 3341 cm^{-1} showed reduced transmittance for CNC40, indicating stronger hydrogen bond cleavage during acid hydrolysis. The C–O–C (1159 cm^{-1}) and C–O (1203 cm^{-1}) bands also displayed noticeable fluctuations, suggesting the partial degradation of glycosidic linkages, particularly at moderate acid concentrations. In contrast, the C–H (2900 cm^{-1}) and aromatic C–C bands (1427 and 1415 cm^{-1}) remained relatively stable, indicating resistance to acid-induced structural damage.

So *et al.* (2021) also reported similar results in FTIR analysis of cellulose extracted from Gelidium amansii using CNC extraction, where cellulose functional groups were found at wavenumbers 2892-2930, 1369, 1315, 1160, and 1054 cm^{-1}. The discovery of this wavenumber indicates the successful isolation of CNC from *Gelidium amansii*.

CNC30, CNC40, CNC50, and CNC60 showed lower transmission values than *Sargassum* sp. at wave numbers 1427, 1415, and 1203 cm^{-1}, which correspond to the aromatic CC and C-O functional groups that make up the lignin structure. Lower transmission values at this number of waves indicate a higher content of the aromatic functional groups CC and C in the sample. This phenomenon can occur due to changes in the structure of lignin that remain during sulfuric acid treatment, where the reactive aromatic ring of lignin is condensed to form a C-C bond, making lignin denser and less soluble in acid (Naufala & Pandebesie, 2015)

Cristallinity of CNC

XRD analysis was performed to determine the CNC crystallinity index. Peaks with maximum intensity are associated

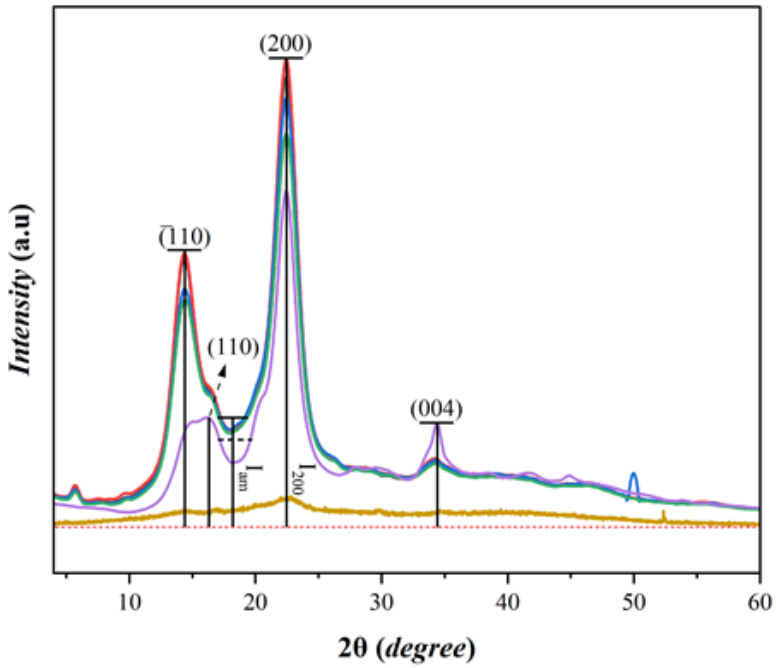

Figure 4 Diffractogram of CNC commercial and CNC extracted from *Sargassum* sp. under different sulfuric acid hydrolysis conditions.
Note: (—)CNC30, (—)CNC40, (—)CNC50, (—)CNC60 are cellulose nanocrystals obtained by 30%, 40%, 50%; 60% sulfuric acid hydrolysis; (—) commercial CNC and (—) *S. polycystum*

with crystalline peaks, whereas those with minimum intensity are associated with the presence of amorphous regions (Suciyati *et al.,* 2022).

Based on Figure 4, *Sargassum* sp. has a wider peak in X-ray diffraction than the other samples. This is due to the high lignin and hemicellulose contents of the sample (Doh *et al.,* 2020; Holilah *et al.,* 2021; Xu & Wang, 2015).

Commercial CNC exhibited amorphous regions between the peaks at 22.4° (200) and 16° (110), whereas all CNC samples from *Sargassum* sp. indicated the presence of amorphous regions between the peaks at 22.4° (200) and 14° ($1\bar{1}0$). The amorphous region of all samples was observed at $2\theta = 18°$. The sample crystallinity index was calculated using the Segal method, and the results are presented in Table 2.

Based on Table 2, the highest crystallinity index was obtained for the commercial CNC at 79.1%. However, the peak intensity of the commercial CNC diffraction at $2\theta = 22.4°$ was lower than that of CNC30, CNC40, CNC50, and CNC60. This phenomenon can occur because of the smaller size of commercial CNCs, resulting in a wider X-ray diffraction peak with a lower peak intensity. This is in line with the statement by Sehe *et al. (*2017), who stated that smaller crystals produce a wider peak in X-ray diffraction, while larger crystals with a single orientation result in a peak of X-ray diffraction closer to the vertical line.

Commercial CNC produced lower peaks at $2\theta = 22.4°$, but the peaks were still relatively sharp with lower amorphous intensities compared to CNC30, CNC40, CNC50, and CNC60. This indicates the high content of cellulose crystals in commercial CNC. This is in accordance with Septriani & Muldarisnur (2022), who stated that low noise (amorphous) and sharp crystal peaks are indicators of the high crystallinity of nanoparticles.

CNC from *Sargassum* sp. showed a fairly high crystallinity index, and the highest crystallinity index was obtained after 40% H_2SO_4 treatment. A high crystallinity index indicates the success of the extraction process in removing the amorphous part of the cellulose chain (El Achaby et al.,2018). CNC was extracted from *Sargassum* sp. using 30% H_2SO_4 exhibited a crystallinity index lower than 40%. These results are in line with the research of Rahmi *et al.* (2023), who showed that the crystallinity index of *cellulose from I. cylindrica treated* with 20% and 30% H_2SO_4 was lower than that of cellulose treated with 40% H_2SO_4. A lower crystallinity index occurs because the low concentration of H_2SO_4 (≤ 30%) could not been able to degrade the amorphous part of the cellulose crystalline.

The crystallinity index that decreased in the treatment with 50% H_2SO_4 and 60% H_2SO_4 indicates the degradation of crystalline cellulose due to excessively high H_2SO_4 concentrations. Rahmi *et al.* (2023) also showed that the cellulose crystallinity index of *Imperata cylindrica* decreased by 50% after H_2SO_4 treatment. This decrease in the crystallinity index occurs because high

Table 2 Crystallinity index of CNC commercial and CNC extracted from *Sargassum* sp. under different sulfuric acid hydrolysis conditions

Sample	2θ (200) (°)		2θ (amorphous) (°)		Cristallinity index (%)
	Degree	I_{200}	Degree	I_{am}	
CNC30	22.43	12.163	18.12	2.789	77.0
CNC40	22.43	12.638	18.10	2.826	77.6
CNC50	22.43	11.686	18.12	2.868	75.4
CNC60	22.45	10.592	18.14	2.753	74.0
Commercial CNC	22.45	9.192	18.28	1.919	79.1

Note: CNC 30, 40, 50, and 60 are cellulose nanocrystals obtained by 30%, 40%, 50% dan 60% sulfuric acid hydrolysis

http://dx.doi.org/10.17844/y5x3as39

concentrations of H_2SO_4 (≥ 50%) can degrade cellulose crystalline and cellulose interchain hydrogen bonds, resulting in low cellulose crystallinity.

The crystallinity of the samples indicates that they are suitable for nanomaterials, as they are in the range of 54-88%. This is in accordance with the statement of Gorbunova *et al*. (2023), who stated that the range of CNC crystallinity index as a nanomaterial amplifier for biocomposites is 54-88%. H_2SO_4 40% was the most effective concentration for extracting CNC from *Sargassum* sp. because it produced the highest crystallinity index. Nanocellulose with a high crystallinity index has a more regular and dense crystal arrangement, resulting in a strong and rigid structure. This structure allows the use of CNC as a reinforcing nanomaterial (Fadly *et al.* 2019).

Thermal Analysis of CNC

TGA was performed to determine the thermal stability of the sample by measuring the changes in the mass of the sample over time and temperature (Apriyanti *et al.,* 2024). An increase in temperature triggers physical and chemical changes in the sample, resulting in mass changes over time (Hu *et al.*, 2014). The thermogravimetric analysis of commercial CNC and CNC extracted from *Sargassum* sp. under different acid hydrolysis conditions is shown in Figure 5.

Based on Figure 5, two stages of decomposition were found in all the analyzed samples, where the first stage of decomposition occurred at temperatures below 100°C, while the second stage of decomposition occurred in the temperature range of 250-390°C. The decomposition of samples below 100 °C indicates the evaporation of absorbed water and low-molecular-weight compounds adsorbed on the surface of the material (Nurazzi *et al.,* 2021). Cellulose decomposes at 300°C, whereas lignin decomposes at 400°C (Henrique *et al.,* 2015). Hemicellulose decomposes at 220 °C (Escalante *et al.,* 2022). The details of the initial decomposition temperature (Tonset), maximum decomposition temperature (Tmax), and residue CNC commercial and CNC extracted from *Sargassum* sp. under different acid hydrolysis conditions are presented in Table 3.

Based on Table 3, *Sargassum* sp. had the lowest initial decomposition temperature (Tonset) among the other samples, at approximately 254°C. This is due to the presence of hemicelluloses. Hemicellulose decomposes at 220°C (Escalante *et al.,* 2022). The acetyl group in hemicellulose can weaken the intermolecular bonds, making hemicellulose decompose more easily at lower temperatures, which contributes to the weight loss of the sample (Hu *et al.*, 2014). Commercial CNC, CNC30, CNC40, CNC50, and CNC60 had a higher Tonset than *Sargassum* sp., at approximately 280-300°C. This indicates the occurrence of a cellulose decomposition process consisting of several simultaneous processes, such as dehydration, depolymerization, and decomposition of glycosidic units (Henrique *et al.,* 2015).

CNC40, CNC50, and CNC60 had lower Tonset values than CNC30. This is related to the concentration of sulfuric acid used during hydrolysis. Higher acid concentrations cause cellulose to be hydrolyzed into smaller sizes (Muljani *et al.,* 2023). Smaller particle sizes have a high surface area and lower heat resistance (Marwanto *et al.,* 2021).

Sargassum sp. has two peaks of maximum decomposition temperature (Tmax) at 270°C and 336°C, which indicate the decomposition of hemicellulose, crystalline cellulose, and cellulose pyrolysis. Commercial CNC, CNC30, CNC40, CNC50, and CNC60 exhibited a single Tmax (sharp peak) at 319-369°C, indicating the acquisition of crystalline cellulose with high purity. This is supported by Bashar *et al*. (2019) research on thermal analysis of burlap fibers which showed three peaks of maximum temperature at 285, 342, and 451°C, which correlated with the decomposition of hemicellulose, crystalline cellulose, cellulose pyrolysis, and lignin, while the CNC sample showed only one peak at a maximum decomposition temperature of 305-318°C, proving the acquisition of crystalline cellulose with high purity.

Commercial CNC exhibited sharp DTG peaks at a maximum decomposition

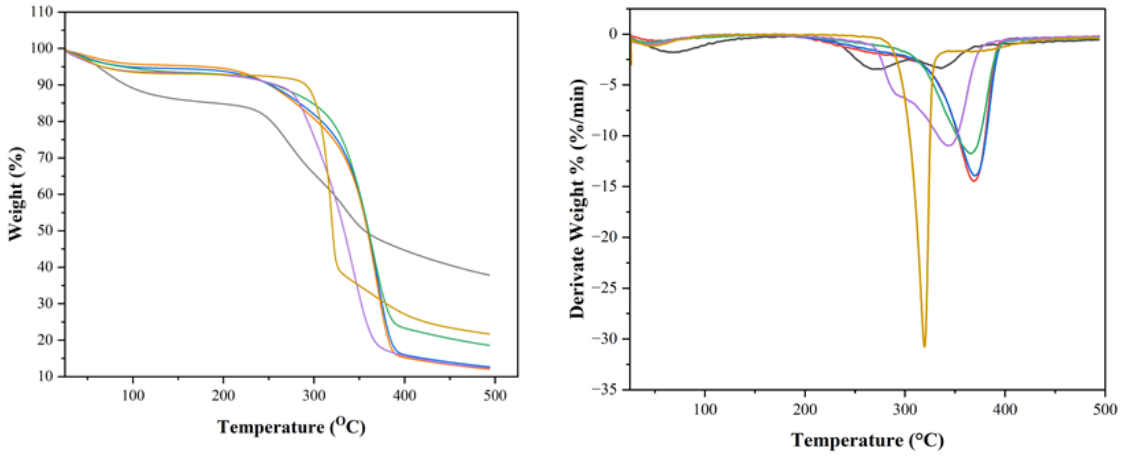

(A) (B)

Figure 5 Thermogravimetric analysis of CNC commercial and CNC extracted from *Sargassum* sp. under different sulfuric acid hydrolysis conditions: (A) Thermogravimetric (TG) % weight; (B) Derivative thermogravimetric (DTG). Note: (—) *S. polycystum*, (—) CNC30, (—) CNC40, (—) CNC50, (—) CNC60 are cellulose nanocrystals obtained by 30%, 40%, 50%; 60% sulfuric acid hydrolysis; and (—) commercial CNC

Table 3 Tonset, Tmax, and percentage of residue of CNC commercial and CNC extracted from *Sargassum* sp. under different sulfuric acid hydrolysis conditions

Sample	Tonset (°C)	Tmax (°C)	Residue (%)
Sargassum sp.	254.18	270.23 336.99	39.43
CNC30	336.30	367.85	15.95
CNC40	332.76	369.60	15.86
CNC50	332.87	366.45	23.19
CNC60	283.28	343.30	16.67
Commercial CNC	307.00	319.16	37.00

Note: CNC 30, 40, 50, and 60 are cellulose nanocrystals obtained by 30%, 40%, 50% dan 60% sulfuric acid hydrolysis

temperature of approximately 319°C, which was lower than those of the Sargassum sp. samples, CNC30, CNC40, CNC50, and CNC60. El Achaby *et al.* (2018) also showed that the maximum decomposition temperature of CNC was lower than *that of Gelidium sesquipedale*. This may be due to the presence of sulfate groups on the CNC surface, which can reduce the thermal stability of the CNC. Bashar *et al.* (2019) stated that the smaller particle size and higher specific surface area of CNC, as well as the presence of more active surface groups, led to lower heat resistance.

The CNC30, CNC50, and CNC60 samples exhibited Tmax values lower than that of CNC40. This can occur due to the lower crystallinity index and the possibility of replacing the hydroxyl group with a sulfuric acid group (O-SO3H) during the acid hydrolysis process. The replacement of these groups lowers the activation energy for CNC decomposition, making the sample less resistant to the pyrolysis. This results in a dehydration reaction that accelerates decomposition at lower temperatures (Costa *et al.,* 2015).

http://dx.doi.org/10.17844/y5x3as39

The CNC40 sample had the highest maximum decomposition temperature compared to the others because it had a higher crystallinity index. A higher crystallinity index indicates greater heat resistance and increases the maximum decomposition temperature (Kazharska *et al.,* 2019). A 40% sulfuric acid concentration is likely the most effective for extracting CNC from *Sargassum* sp. because it has a higher maximum decomposition temperature than other concentrations.

The highest residue percentage was obtained for S. *polycystum*, which was approximately 39%. Singh *et al*. (2017) also showed that *Gelidiella acerosa* has a higher residue than CNC, which is 30%.

Cristallin Size of CNC

X-ray diffraction (XRD) analysis revealed a clear trend in the Full Width at Half Maximum (FWHM) and crystallite size of the CNC samples hydrolyzed using different concentrations of sulfuric acid (30%, 40%, 50%, and 60%). The CNC 30% sample exhibited the narrowest FWHM value (8.57°), corresponding to the highest crystallite size among the synthesized samples (approximately 0.94 nm). In contrast, the CNC 40%, 50%, and 60% samples showed broader diffraction peaks with FWHM values exceeding 8.85° and slightly reduced crystallite sizes in the range of 0.90–0.91 nm. This trend suggests that higher concentrations of sulfuric acid induce more extensive hydrolysis, leading to the fragmentation of the crystalline regions of cellulose.

As a result, the crystallites formed were smaller and more structurally disordered, consistent with previous studies indicating that intense acid hydrolysis increases the amorphous fraction of cellulose nanocrystals (Beck-Candanedo *et al.,* 2005; Gray, 2013).

In contrast, the commercial CNC sample exhibited a remarkably narrower FWHM of 1.22° and a significantly larger crystallite size of 6.61 nm than the synthesized CNCs. This indicates a higher degree of crystallinity, likely due to differences in raw material purity, process control, and post-treatment techniques used in industrial production. Commercially produced CNCs are typically derived from highly purified cellulose sources and may undergo optimized hydrolysis and stabilization procedures, which help preserve and promote the development of larger crystalline domains. This high crystallinity enhances the mechanical strength, thermal stability, and optical clarity of CNC, making them ideal for advanced applications such as nanocomposites, coatings, and biomedical materials (Habibi *et al.,* 2010; Moon *et al.,* 2011; Wang *et al.,* 2007).

The crystallinity index achieved by CNC from Sargassum sp. (up to 77.6%) and its high thermal stability (Tmax up to 369.60°C) demonstrate characteristics that are in line with the criteria for such applications (Habibi *et al.,* 2010; Moon *et al.,* 2011). Although the crystallite size was relatively small (0.90–0.94 nm), it still fell within the acceptable range used in nanocomposite material formulations. However, further characterization, including

Table 4 Crystalline size of CNC commercial and CNC extracted from *Sargassum* sp. under under different sulfuric acid hydrolysis conditions

Sample	FWHM (°)	Crystalline size(nm)
Sargassum sp.	-	-
CNC30	8.5731	0.94
CNC40	8.9609	0.90
CNC50	8.8589	0.91
CNC60	8.9813	0.90
Commercial CNC	1.2247	6.61

Note: CNC 30, 40, 50, and 60 are cellulose nanocrystals obtained by 30%, 40%, 50% dan 60% sulfuric acid hydrolysis

morphological analysis, surface charge, and dispersion stability, is required to confirm its suitability for specific applications.

CONCLUSION

FTIR analysis confirmed the reduction of lignin and hemicellulose in the CNC of *Sargassum* sp. after delignification and bleaching treatment. XRD analysis showed that CNC had higher crystallinity than the raw materials, while TGA showed better thermal stability. Hydrolysis with 30% sulfuric acid was effective in producing CNC with a high crystallinity index (77.6%) and significant thermal stability (Tmax = 369.60°C). Treatment with varying sulfuric acid concentrations had no significant effect on the crystallite size of the CNC. The crystallite size remained within the narrow range of 0.90–0.94 nm. These findings highlight the potential of *Sargassum* sp. as a valuable resource for CNC production, contributing to its utilization as a nanomaterial in a wide range of applications.

ACKNOWLEDGEMENTS

This research was supported by PUTI HIBAH PASCA with grant number NKB-119/UN2. RST/HKP.05.00/2024 by Prof. Dr. Dedi Priadi.

REFERENCE

Abu-Thabit, N. Y., Judeh, A. A., Hakeem, A. S., Ul-Hamid, A., Umar, Y., & Ahmad, A. (2020). Isolation and characterization of microcrystalline cellulose from date seeds (*Phoenix dactylifera L.*). *International Journal of Biological Macromolecules*, 155(1), 730–739. https://doi.org/10.1016/j.ijbiomac.2020.03.255

Agustin, D. A., & Wibowo, A. A. (2021). Teknologi enkapsulasi: teknik dan aplikasinya. *Distilat: Jurnal Teknologi Separasi*, 7(2), 202–209.

Alam, M. K., Hossain, M. S., Bahadur, N. M., & Ahmed, S. (2024). A comparative study in estimating of crystallite sizes of synthesized and natural hydroxyapatites using Scherrer method, Williamson-Hall model, Size-Strain Plot and Halder-Wagner Method. *Journal of Molecular Structure*, 1306. https://doi.org/10.1016/j.molstruc.2024.137820

Apriyanti, E., Chasanah, U., & Subekti, S. (2024). Pengembangan metode filtrasi menggunakan membran keramik berbasis *fly ash* batubara. PT. Sonpedia Publishing Indonesia.

Bashar, M. M., Zhu, H., Yamamoto, S., & Mitsuishi, M. (2019). Highly carboxylated and crystalline cellulose nanocrystals from jute fiber by facile ammonium persulfate oxidation. *Cellulose*, 26(6), 3671–3684. https://doi.org/10.1007/s10570-019-02363-7

Beck-Candanedo, S., Roman, M., & Gray, D. G. (2005). Effect of reaction conditions on the properties and behavior of wood cellulose nanocrystal suspensions. *Biomacromolecules*, 6(2), 1048–1054. https://doi.org/10.1021/bm049300p

Costa, L. A. D. S., Fonseca, A. F., Pereira, F. V, & Druzian, J. I. (2015). Extraction and characterization of cellulose nanocrystals from corn stover. *Cellulose Chemistry and Technology*, 49(2), 127–133.

Doh, H., Lee, M. H., & Whiteside, W. S. (2020). Physicochemical characteristics of cellulose nanocrystals isolated from seaweed biomass. *Food Hydrocolloids*, 102. https://doi.org/10.1016/j.foodhyd.2019.105542

Doh, H., & Whiteside, W. S. (2020). Isolation of cellulose nanocrystals from brown seaweed, *Sargassum fluitans*, for development of alginate nanocomposite film. *Polymer Crystallization*, 3(4), 1–10. https://doi.org/10.1002/pcr2.10133

El Achaby, M., Kassab, Z., Aboulkas, A., Gaillard, C., & Barakat, A. (2018). Reuse of red algae waste for the production of cellulose nanocrystals and its application in polymer nanocomposites. *International Journal of Biological Macromolecules*, 106(1), 681–691. https://doi.org/10.1016/j.ijbiomac.2017.08.067

Erniati, Syahrial, Erlangga, Imanullah, & Andika, Y. (2024). Aktivitas antioksidan dan total fenol *Sargassum* sp. dari Perairan Simeulue Aceh. *Jurnal Pengolahan Hasil Perikanan*

Indonesia, 27(3), 186-196. http://dx.doi.org/10.17844/jphpi.v27i3.46981

Escalante, J., Chen, W. H., Tabatabaei, M., Hoang, A. T., Kwon, E. E., Lin, K. Y. A., & Saravanakumar, A. (2022). Pyrolysis of lignocellulosic, algal, plastic, and other biomass wastes for biofuel production and circular bioeconomy: A review of thermogravimetric analysis (TGA) approach. *Renewable and Sustainable Energy Reviews*, 169(1), 1–21. https://doi.org/10.1016/j.rser.2022.112914

Fadly, C. C., Evelyna, A., & Sunendar, B. (2019). Efek penambahan nanoselulosa terhadap compressive strength bone cement berbasis kalsium fosfat. *SONDE (Sound of Dentistry)*, 3(2), 98–107. https://doi.org/10.28932/sod.v3i2.1786

Fransiska, D., Akbar, R., & Giyatmi. (2020). Karakterisasi natrium alginat dari Banten, Lampung, dan Yogyakarta. *Jurnal Teknologi Pangan Kesehatan*, 2(2), 97–104.

George, J., & Sabapathi, S. N. (2015). Cellulose nanocrystals: Synthesis, functional properties, and applications. *Nanotechnology, Science and Applications*, 8(1), 45–54. https://doi.org/10.2147/NSA.S64386

Gian, A. A., Farid, M., & Ardhyananta, H. (2017). Isolasi selulosa dari serat tandan kosong kelapa sawit untuk nano filter komposit absorpsi suara: analisis FTIR. *Jurnal Teknik ITS*, 6(2), 228–231.

Gorbunova, M., Grunin, L., Morris, R. H., & Imamutdinova, A. (2023). Nanocellulose-based thermoplastic polyurethane biocomposites with shape memory effect. *Journal of Composites Science*, 7(4), 1–43. https://doi.org/10.3390/jcs7040168

Gray, D. (2013). Nanocellulose: from nature to high performance tailored material. *Holzforschung*, 67(3), 353-353.. https://doi.org/doi:10.1515/hf-2013-0027

Habibi, Y., Lucia, L. A., & Rojas, O. J. (2010). Cellulose nanocrystals: chemistry, self-assembly, and applications. *Chemical reviews*, 110(6), 3479–3500. https://doi.org/10.1021/cr900339w

Harahap, H., Harfansah Nst, A., & Fujian Junaidi, I. (2019). Pengaruh konsentrasi asam sulfat (H_2S_O4) pada hidrolisa tongkol jagung (*Zea mays*) menjadi nanokristal selulosa sebagai filler penguat pada produk lateks karet alam. *Jurnal Teknik Kimia USU*, 8(2), 48–53. https://doi.org/10.32734/jtk.v8i2.1873

Harpendi, R., Padil, & Yelmida. (2014). Proses pemurnian selulosa pelepah sawit sebagai bahan baku nitrolesulosa dengan variasi pH dan konsentrasi H_2O_2. *Jurnal Online Mahasiswa Fakultas Teknik Universitas Riau*, 1(1), 1–8.

Henrique, M. A., Flauzino Neto, W. P., Silvério, H. A., Martins, D. F., Gurgel, L. V. A., Barud, H. da S., Morais, L. C. de, & Pasquini, D. (2015). Kinetic study of the thermal decomposition of cellulose nanocrystals with different polymorphs, cellulose I and II, extracted from different sources and using different types of acids. *Industrial Crops and Products*, 76(1), 128–140. https://doi.org/10.1016/j.indcrop.2015.06.048

Hikmawati, N., Suprianto, & Ismawati. (2023). Pengaruh minat berwirausaha terhadap pengembangan budidaya rumput laut di Kabupaten Sumbawa. *SAMALEWA (Jurnal Riset Dan Kajian Manajemen)*, 3(2), 218–227.

Holilah, H., Prasetyoko, D., Ediati, R., Bahruji, H., Jalil, A. A., Asranudin, A., & Anggraini, S. D. (2021). Hydrothermal assisted isolation of microcrystalline cellulose from pepper (*Piper nigrum L.)* processing waste for making sustainable bio-composite. *Journal of Cleaner Production*, 305(1), 1–15. https://doi.org/10.1016/j.jclepro.2021.127229

Hu, Y., Tang, L., Lu, Q., Wang, S., Chen, X., & Huang, B. (2014). Preparation of cellulose nanocrystals and carboxylated cellulose nanocrystals from borer powder of bamboo. *Cellulose*, 21(3), 1611–1618. https://doi.org/10.1007/s10570-014-0236-0

Kazharska, M., Ding, Y., Arif, M., Jiang, F., Cong, Y., Wang, H., Zhao, C., Liu, X., Chi, Z., & Liu, C. (2019). Cellulose nanocrystals derived from *Enteromorpha prolifera* and their use in

developing bionanocomposite films with water-soluble polysaccharides extracted from *E. prolifera*. *International Journal of Biological Macromolecules*, 134(1), 390–396. https://doi.org/10.1016/j.ijbiomac.2019.05.058

Khansa, H. H., Sari, R. P., & Agitha, S. R. A. (2024). Uji organoleptik dan daya hambat ekstrak alga coklat (*Sargassum polycystum*) terhadap jamur *Candida albicans*. *Surabaya Bomedical Journal*, 3(2), 142–152.

Kusumaningsih, T., Masykur, A., & Aninditha, A. S. (2022). Preparation and characterization of PVA/Na-CMC hydrogel from OPEFB cross-linked by maleic anhydride. *EduChemia Jurnal Kimia Dan Pendidikan*, 7(1), 36–55. https://doi.org/10.30870/educhemia.v7i1.12637

Marwanto, M., Maulana, M. I., Febrianto, F., Wistara, N. J., Nikmatin, S., Masruchin, N., Zaini, L. H., Lee, S. H., & Kim, N. H. (2021). Characteristics of nanocellulose crystals from balsa and kapok fibers at different ammonium persulfate concentrations. *Wood Science and Technology*, 55(5), 1319–1335. https://doi.org/10.1007/s00226-021-01319-0

Moon, R. J., Martini, A., Nairn, J., Simonsen, J., & Youngblood, J. (2011). Cellulose nanomaterials review: structure, properties and nanocomposites. *Chemical Society Reviews*, 40(7), 3941–3994. https://doi.org/10.1039/C0CS00108B

Moranda, D. P., Handayani, L., & Nazlia, S. (2018). Pemanfaatan limbah kulit ikan tuna sirip kuning (*Thunnus albacares*) sebagai gelatin: Hidrolisis menggunakan pelarut HCl dengan konsentrasi berbeda. *Acta Aquatica: Aquatic Sciences Journal*, 5(2), 81–87. https://doi.org/10.29103/aa.v5i2.850

Muljani, S., Candra, A., & Faiqoh, I. (2023). Sintesis dan karakterisasi selulosa kristal dari batang tembakau. *Jurnal Teknik Kimia*, 17(2), 46–51. https://doi.org/10.33005/jurnal_tekkim.v17i2.3780

Murugesan, S., R, R. R. S., & Rajan, R. (2024). Extraction and characterization of cellulose nanocrystals from brown seaweed *Dictyota bartayreisana*, J.V.Lamouroux. *Research Square*, 1-15. https://doi.org/10.21203/rs.3.rs-4099221/v1 (Under review)

Natsir, Muh., Pratiwi, A. M., Azis, T., Nohong, I., Harlis, W. O., Alimin, Kadidae, L. O., Ruslan C., B., Kadir, L. O. A., & Nurliana, L. (2022). Efektivitas fotodegradasi lignin dari limbah ampas sagu (*Metroxylon sagu Rottb.*) menggunakan katalis TiO_2. *KOVALEN: Jurnal Riset Kimia*, 8(3), 258–265. https://doi.org/10.22487/kovalen.2022.v8.i3.16149

Naufala, W. A., & Pandebesie, E. S. (2015). Hidrolisis eceng gondok dan sekam padi untuk menghasilkan gula reduksi sebagai tahap awal produksi bioetanol. *Jurnal Teknik ITS*, 4(2), 109–113.

Nurazzi, N. M., Asyraf, M. R. M., Rayung, M., Norrrahim, M. N. F., Shazleen, S. S., Rani, M. S. A., Shafi, A. R., Aisyah, H. A., Radzi, M. H. M., Sabaruddin, F. A., Ilyas, R. A., Zainudin, E. S., & Abdan, K. (2021). Thermogravimetric analysis properties of cellulosic natural fiber polymer composites: A review on influence of chemical treatments. *Polymers*, 13(16), 2710; https://doi.org/10.3390/polym13162710

Nurhayati, Irianto, H. E., Supriyanto, A., Kusumawati, R., Basmal, J., Munifah, I., Setiawati, N. P., Kusumaningrum, W. B., Amanda, P., Roziafanto, A. N., Riastuti, R., & Chalid, M. (2025). View of isolation and characterization of cellulose microfibril (MFC) from *Gracilaria* sp. with different quality grades. *Science & Technology Indonesia*, 10(3), 712–724. https://doi.org/https://doi.org/10.26554/sti.2025.10.3.712-724

Pambudi, A., Farid, Moh., & Nurdiansah, H. (2017). Analisis morfologi dan spektroskopi infra merah serat bambu bentung (*Dendrocalamus asper*) hasil proses alkalisasi sebagai penguat komposit absorbsi suara. *Jurnal Teknik ITS*, 6(2), 441–444. https://doi.org/10.12962/j23373539.v6i2.24808

Pangau, J. R., Sangian, H. F., & Lumi, B. M. (2017). Karakterisasi bahan selulosa

dengan iradiasi pretreatment gelombang mikro terhadap serbuk kayu cempaka wasian (*Elmerillia ovalis*) di Sulawesi Utara. *Jurnal MIPA,* 6(1), 53–58. https://doi.org/10.35799/jm.6.1.2017.16157

Pine, A. T. D., Base, N. H., & Angelina, J. B. (2021). Produksi dan karakterisasi serbuk selulosa dari batang pisang (*Musa paradisiaca L.*). *Jurnal Kesehatan Yamasi Makassar*, 5(2), 115–120.

Plianwong, S., & Sirirak, T. (2024). Cellulose nanocrystals from marine algae *Cladophora glomerata* by using microwave-assisted extraction. *International Journal of Biological Macromolecules*, 260. https://doi.org/10.1016/j.ijbiomac.2024.129422

Rahmi, Lubis, S., Adlim, M., Lelifajri, Zahra, N. A., & Fathana, H. (2023). Pemanfaatan Selulosa dari Bahan Alam Pada Pembuatan Komposit Kitosan. Syiah Kuala University Press.

Ramlan, Prangdimurti, E., Adawiyah, D. R., & Nurjanah. (2024). Karakteristik fisikokimia dan fungsional tepung *Sargassum polycystum* sebagai bahan baku pembuatan garam fungsional. *Jurnal Pengolahan Hasil Perikanan Indonesia*, 27(11), 1050-1073. http://dx.doi.org/10.17844/jphpi.v27i11.59103

Raturandang, R., Wenas, D. R., Mongan, S., & Bujung, C. (2022). Analisis spektroskopi FTIR untuk karakterisasi kimia fisik fluida mata air panas di kawasan wisata hutan pinus Tomohon Sulawesi Utara. *Jurnal FisTa: Fisika Dan Terapannya*, 3(1), 28–33. https://doi.org/10.53682/fista.v3i1.167

Safitri, I., Warsidah, Sofiana, M. S. J., Kushadiwijayanto, A. A., & Sumarni, T. N. (2021). Total phenolic content, antioxidant and antibacterial activities of *Sargassum polcystum* of ethanol extract from wasters of Kabung Island. *Berkala Sainstek*, 9(3), 139–145. https://doi.org/10.19184/bst.v9i3.27199

Saputri, L. H., & Sukmawan, R. (2020). Pengaruh proses blending dan ultrasonikasi terhadap struktur morfologi ekstrak serat limbah batang kelapa sawit untuk bahan baku bioplastik (selulosa asetat). *Rekayasa*, 13(1), 15–21. https://doi.org/10.21107/rekayasa.v13i1.6180

Sehe, M. Ri., Sangian, H. F., & Tongkukut, S. H. J. (2017). Studi perbandingan struktur selulosa dengan pretreatment larutan ion pada kayu cempaka (*Elmerillia ovalis*). *Jurnal MIPA*, 7(1), 1–4. https://doi.org/10.35799/jm.7.1.2018.18806

Septiani, E., Pratama, G., & Putri, R. M. S. (2017). Ekstraksi Na-alginat dari rumput laut Padina sp. menggunakan konsentrasi kalium hidroksida yang berbeda. *Biosfera*, 34(3), 110–116. https://doi.org/10.20884/1.mib.2017.34.3.500

Septriani, Y., & Muldarisnur, M. (2022). Kontrol ukuran nanopartikel perak dengan variasi konsentrasi ekstrak kulit buah manggis. *Jurnal Fisika Unand*, 11(1), 68–74. https://doi.org/10.25077/jfu.11.1.68-74.2022

Simarmata, R. T. B., Johan, V. S., Dewi, Y. K., Yunita, I., & Kurniawan, M. A. (2024). Pembuatan plastik biodegradable berbahan dasar pati bonggol pisang dengan selulosa jerami padi. *Jurnal Agroindustri Halal*, 10(1), 23–32.

Singh, S., Gaikwad, K. K., Park, S. Il, & Lee, Y. S. (2017). Microwave-assisted step reduced extraction of seaweed (*Gelidiella aceroso*) cellulose nanocrystals. *International Journal of Biological Macromolecules*, 99, 506–510. https://doi.org/10.1016/j.ijbiomac.2017.03.004

So, B. R., Yeo, H. J., Lee, J. J., Jung, Y. H., & Jung, S. K. (2021). Cellulose nanocrystal preparation from *Gelidium amansii* and analysis of its antiinflammatory effect on the skin in vitro and in vivo. *Carbohydrate Polymers*, 254(1), 117315.

Suciyati, S. W., Manurung, P., Junaidi, & Situmeang, R. (2022). Efek variasi konsentrasi NaOH pada pembentukan struktur selulosa *Clodophora* sp. *Jurnal Teori dan Aplikasi Fisika*, 10(1), 11–24.

Sunardi, Lestari, A., Junaidi, A. B., & Istikowati, W. T. (2019). Isolation of microcrystalline cellulose from medang wood (*Neolitsea latifolia*). *Konversi*, 8(2), 69–76. https://doi.org/10.20527/k.v8i2.6839

Taslim, M., Mailoa, M., & Rijal, M. (2017). Pengaruh pH, dan lama fermentasi terhadap produksi ethanol dari *Sargassum crassifolium*. *Biosel: Biology Science and Education*, 6(1), 13–25. https://doi.org/10.33477/bs.v6i1.129

Theivandran, G., Ibrahim, S. M., & Murugan, M. (2015). Fourier transform infrared (Ft-Ir) spectroscopic analysis of *Spirulina fusiformis*. *Journal of Medicinal Plants Studies*, 3(4), 30–32.

Topală, C. M., Tătaru, L. D., & Ducu, C. (2017). ATR-FTIR spectra fingerprinting of medicinal herb extracts prepared using microwave extraction. *Arabian Journal of Medicinal and Aromatic Plants*, 3(1), 1–9.

Umpuch, C. (2015). Batch adsorption of organic dyes by organo-bagasse: Carbon content, pH influence, kinetics and isotherms. *International Journal of Engineering, Transactions A: Basics*, 28(4), 507–515. https://doi.org/10.5829/idosi.ije.2015.28.04a.03

Wang, B., Sain, M., & Oksman, K. (2007). Study of structural morphology of hemp fiber from the micro to the nanoscale. *Applied Composite Materials*, 14(2), 89–103. https://doi.org/10.1007/s10443-006-9032-9

Xu, F., & Wang, D. (2015). Analysis of lignocellulosic biomass using infrared methodology. *In Pretreatment of Biomass: Processes and Technologies*,7-25. https://doi.org/10.1016/B978-0-12-800080-9.00002-5